International Journal of Civil And Structural Engineering – IJCSE 2018
Copyright © Institute of Research Engineers and Doctors , SEEK Digital Library
Volume 5 : Issue 2- [ISSN : 2372-3971] - Publication Date: 28 December, 2018

Response of Buildings to Earthquake Loading by Structural Mixture Theory

Mohammed S. Al-Ansari and **Muhammad S. Afzal**

***Abstract*—** The response of a structural frame to earthquake ground motion is predicted using the structural mixture theory (SMT). This research presents four different case studies to evaluate the performance of the structure mixture theory in the earthquake response analysis of buildings. In the first case study, the actual earthquake responses of the two-story reinforced concrete building, which was tested at the University of California at Berkeley, were compared to those obtained using the SMT. In the second case study, the seven-story reinforced concrete building, which was tested as a part of the US-Japan Cooperative Earthquake Program, was considered. The third case study is about the calculation of nodal deflection amplitude with SMT and comparison of the results obtained from Wilson-θ method. In the fourth case study, the observed earthquake response of a nine-story steel frame building during San Fernando earthquake is compared with the SMT numerical results of the structure. All the case studies showed that the structure mixture theory (SMT) results were very close to the experimental and numerical results. The mean differences between the maximum roof displacements obtained experimentally and numerically in all of the four case studies and those obtained using the SMT were found to be equal to 3.5%, 3.2%, 2.4% and 5.6% respectively. The structural mixture theory is valid for multiple-degree-of-freedom structures under the type of ground motions used in this study, and it appears to be applicable to systems with linear or nonlinear behavior.

Keywords*— *Earthquake ground motion, Structure Mixture Theory, nodal deflection amplitude

1. Introduction

Al-Ansari et. al [1] presented a structure mixture theory for the earthquake analysis of two-dimensional structural systems. In this approach, the structural system is considered as mixture of two interacting subsystems: columns and beams/floors. Its own linear differential operator describes the response of each subsystem. The two responses are then subjected to matching boundary conditions, which couple them at the subsystem interface.

Mohammed S. Al-Ansari
Department of Civil and Architectural Engineering, Qatar University
Doha, Qatar

Muhammad Shekaib Afzal
Department of Civil and Architectural Engineering, Qatar University
Doha, Qatar

The solution of the coupled equations is carried out using a pair of perturbation series. The structure mixture technique is an advantageous technique for the earthquake response analysis of two-dimensional buildings because it does not deal with initial conditions and time integration and spectral charts. Moreover, the technique does not require the use of the complete damping matrix for the structure as long as the modal damping ratios are known. During the past 35 years, a number of experimental studies on the behavior of multi-story buildings under earthquake loading were carried out [2-8]. Baiping et. al. [9] investigated experimentally the seismic response and damage of steel moment resisting frame (MRF) building structures with non-liner viscous dampers using ground motions up to and beyond the maximum considered earthquake (MCE) level. These studies have resulted in a better understanding of the behavior of buildings during earthquakes. The studies' data has been utilized in the development of analytical methods as well as codes of practice for the analysis and design of earthquake-resistant buildings [10-13].

Earthquake ground motion is usually measured by a strong motion accelerograph which records the acceleration of the ground at a particular location. The recorded accelerograms, after they are corrected and adjusted, may be integrated to obtain velocity and displacement time histories. Some records of seismic events, such as the San Fernando (1971) and El Centro (1940) earthquakes, are frequently used in earthquake engineering. For more details on the equations of motion and their simultaneous solution. [14], [15]. The actual top drift of the Bank of California building during San Fernando earthquake was accurately predicted using the closed-form response equation [16].

Five simulated models were used to obtain the non-linear response of tall buildings subjected to dynamic and static equivalent load (UBC code) [17].

The earliest design analyses for predicting the response of the structure were based on single degree of freedom (SDOF) model which gives the response in terms of a single displacement coordinate (at the top of a structure). Dynamic analysis techniques were formulated in parallel with matrix methods for static structural analysis, and both were concurrent with development of digital computers which can handle the vast quantities of numerical operations required for the solution of MDOF systems.

The determination of the nonlinear response of MDOF structural models requires a step-by-step numerical integration of the equations of motion (in time). One of the simplest of the many methods available is a modification of the linear

acceleration method, known as the Wilson-θ method [18]. The Wilson- θ method is unconditionally stable, i.e., numerical errors do not tend to accumulate during the integration process, regardless of the selected magnitude of the time step. It is also equally applicable to systems with linear or nonlinear behavior, and is therefore quite convenient to use as a benchmark with which other approaches to the calculation of structural earthquake response may be compared. The bidirectional seismic response of fully base-isolated (FBI) adjacent buildings with different heights and segregated foundations has been studied by Khalid et.al. [19]. Their research study reveals that isolation systems significantly enhances the overall response of base isolated building.

This paper presents a brief description of the structure mixture theory and investigates, using four case studies, its performance in the earthquake response analysis of multi-story buildings. The first case study is concerned with the earthquake responses of the two-story reinforced concrete building, which was tested at the University of California at Berkeley. The second is concerned with the seven-story reinforced concrete building, which was tested as a part of the US-Japan Cooperative Earthquake Program. The third case study is about the calculation of nodal deflection amplitude with SMT and comparison of the results obtained from Wilson- θ method. In the fourth case study, the observed earthquake response of a nine-story steel frame building during San Fernando earthquake [20] is compared with the SMT numerical results of the structure. The simulated earthquake responses of experimental buildings were compared to those obtained using the structure mixture theory.

Structure Mixture Theory Overview

It is always possible to view a building as being composed of two distinct but interlocked structural subsystems. The supporting columns are treated as subsystem 1 while the beams/ floors are treated as subsystem 2. It is possible to represent the effects of subsystem 2 in a relatively simple manner by means of a set of translational (horizontal) and rotational spring stiffeners.

A typical one-story building is modeled as two subsystems as shown in Figure 1. The effect of the beam-column interaction is modeled by a set of stiffeners positioned at the interface as shown in Figure 2.

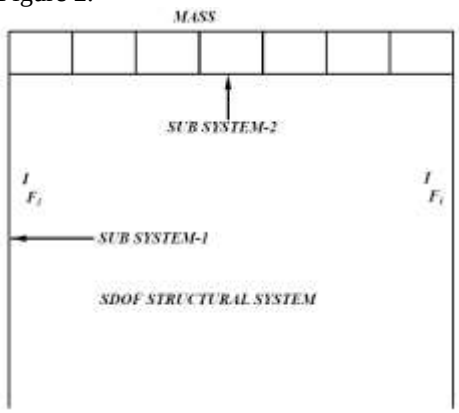

Figure 1: Structure Mixture Frame

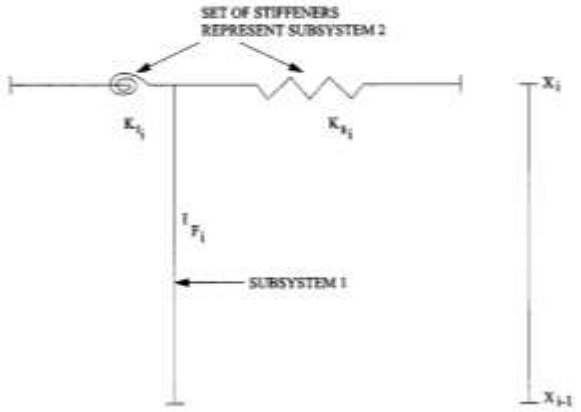

Figure 2: Structure Mixture Theory Model

1) Transverse Dynamic Solution for Subsystem-1 (Columns)

The transverse deflection amplitude of columns is given by the following differential equation:

$$\frac{d^4 y_i}{dx^4} - \kappa_i^4 y_i = 0. \qquad (1)$$

The wave number, κ_i, is given by the following equation:

$$\kappa_i = \sqrt{\frac{\Omega}{c_i r_{g_i}}} \qquad (2)$$

where c_i = bulk wave speed in the column material; Ω = circular (radian) frequency; and rgi = column radius of gyration. The equation for transverse waves in a column is represented by Eq-1. It has been chosen because the earthquake loading at the foundation of the structure is predominantly transverse with respect to the columns. The deflection amplitude of the general column section is given by the following equation (general solution of Eq. 1):

$$y_i = A_i e^{\kappa x} + B_i e^{-\kappa x} + C_i \cos(\kappa x) + D_i \sin(\kappa x) \qquad x_{i-1} \le x \le x_i \qquad (3)$$

where the four constants of integration A_i, B_i, C_i, and D_i are determined by the boundary conditions at x_i and x_{i-1}. The general subscript index "i" represents the column sections between stories in sequence from the ground up (for the Single degree of freedom system under discussion we always have i = 1). For multi-story structures, additional boundary conditions are given at the other interface points x_i (i = 2, 3,…..,n-1) as shown in Figure 2.

The boundary conditions in terms of displacement, slope, shear, and moment at the interface nodes are as follows.

$$\text{At point } x_{i-1} \qquad y_i = \delta_{i-1} \qquad \frac{dy_i}{dx} = \theta_{i-1} \tag{4}$$

$$\text{At point } x_i \qquad E I_{F_i} \frac{d^3 y_i}{dx^3} = k_{s_i}\, \delta_i \qquad E I_{F_i} \frac{d^2 y_i}{dx^2} = k_{t_i}\, \theta_i$$

where δ_i and δ_{i-1} = transverse displacements, θ_i and θ_{i-1} = slopes, k_{si} = translational spring coefficient, k_{ti} = rotational spring coefficient, I_{Fi} = total frame stiffness, and E = elastic modulus.

Combining Eqs. 3 and 4, the following expressions for the constants A_i, B_i, C_i, and D_i are obtained:

$$A_i = \frac{1}{2\psi_i}\left\{\begin{array}{l} \tilde{\delta}_i \begin{bmatrix} e^{-\phi_i} + e^{-\phi_{i-1}} \sin\phi_i \sin\phi_{i-1} + e^{-\phi_{i-1}} \cos\phi_i \sin\phi_{i-1} \\ - e^{-\phi_{i-1}} \sin\phi_i \cos\phi_{i-1} + e^{-\phi_{i-1}} \cos\phi_i \cos\phi_{i-1} \end{bmatrix} \\ + \delta_{i-1} \begin{bmatrix} e^{-\phi_{i-1}} + e^{-\phi_i} \sin\phi_i \sin\phi_{i-1} + e^{-\phi_i} \cos\phi_i \sin\phi_{i-1} \\ - e^{-\phi_i} \sin\phi_i \cos\phi_{i-1} + e^{-\phi_i} \cos\phi_i \cos\phi_{i-1} \end{bmatrix} \\ + \Phi_{i-1} \begin{bmatrix} e^{-\phi_{i-1}} + e^{-\phi_i} \sin\phi_i \sin\phi_{i-1} - e^{-\phi_i} \cos\phi_i \sin\phi_{i-1} \\ + e^{-\phi_i} \sin\phi_i \cos\phi_{i-1} + e^{-\phi_i} \cos\phi_i \cos\phi_{i-1} \end{bmatrix} \\ + \Phi_i \begin{bmatrix} e^{-\phi_i} + e^{-\phi_{i-1}} \sin\phi_i \sin\phi_{i-1} - e^{-\phi_{i-1}} \cos\phi_i \sin\phi_{i-1} \\ + e^{-\phi_{i-1}} \sin\phi_i \cos\phi_{i-1} + e^{-\phi_{i-1}} \cos\phi_i \cos\phi_{i-1} \end{bmatrix} \end{array}\right\} \tag{5}$$

$$B_i = \frac{1}{2\psi_i}\left\{\begin{array}{l} \tilde{\delta}_i \begin{bmatrix} - e^{\phi_i} - e^{\phi_{i-1}} \sin\phi_i \sin\phi_{i-1} + e^{\phi_{i-1}} \cos\phi_i \sin\phi_{i-1} \\ - e^{\phi_{i-1}} \sin\phi_i \cos\phi_{i-1} - e^{\phi_{i-1}} \cos\phi_i \cos\phi_{i-1} \end{bmatrix} \\ + \delta_{i-1} \begin{bmatrix} e^{\phi_{i-1}} + e^{\phi_i} \sin\phi_i \sin\phi_{i-1} - e^{\phi_i} \cos\phi_i \sin\phi_{i-1} \\ + e^{\phi_i} \sin\phi_i \cos\phi_{i-1} + e^{\phi_i} \cos\phi_i \cos\phi_{i-1} \end{bmatrix} \\ + \Phi_{i-1} \begin{bmatrix} - e^{\phi_{i-1}} - e^{\phi_i} \sin\phi_i \sin\phi_{i-1} - e^{\phi_i} \cos\phi_i \sin\phi_{i-1} \\ + e^{\phi_i} \sin\phi_i \cos\phi_{i-1} - e^{\phi_i} \cos\phi_i \cos\phi_{i-1} \end{bmatrix} \\ + \Phi_i \begin{bmatrix} e^{\phi_i} + e^{\phi_{i-1}} \sin\phi_i \sin\phi_{i-1} + e^{-\phi_{i-1}} \cos\phi_i \sin\phi_{i-1} \\ - e^{\phi_{i-1}} \sin\phi_i \cos\phi_{i-1} + e^{\phi_{i-1}} \cos\phi_i \cos\phi_{i-1} \end{bmatrix} \end{array}\right\} \tag{6}$$

$$C_i = \frac{1}{2\psi_i}\left\{\begin{array}{l} \tilde{\delta}_i \begin{bmatrix} 2\sin\phi_i + e^{(\phi_i - \phi_{i-1})} \sin\phi_{i-1} + e^{(\phi_i - \phi_{i-1})} \cos\phi_{i-1} \\ + e^{(\phi_{i-1} - \phi_i)} \sin\phi_{i-1} - e^{(\phi_{i-1} - \phi_i)}{}_i \cos\phi_{i-1]} \end{bmatrix} \\ + \delta_{i-1} \begin{bmatrix} -2\cos\phi_{i-1} - e^{(\phi_i - \phi_{i-1})} \sin\phi_i + e^{(\phi_i - \phi_{i-1})} \cos\phi_i \\ + e^{(\phi_{i-1} - \phi_i)} \sin\phi_i + e^{(\phi_{i-1} - \phi_i)} \cos\phi_i \end{bmatrix} \\ + \Phi_{i-1} \begin{bmatrix} -2\sin\phi_{i-1} - e^{(\phi_i - \phi_{i-1})} \sin\phi_i - e^{(\phi_i - \phi_{i-1})} \cos\phi_i \\ - e^{(\phi_{i-1} - \phi_i)} \sin\phi_i - e^{(\phi_{i-1} - \phi_i)} \cos\phi_i \end{bmatrix} \\ + \Phi_i \begin{bmatrix} -2\cos\phi_i - e^{(\phi_i - \phi_{i-1})} \sin\phi_{i-1} - e^{(\phi_i - \phi_{i-1})} \cos\phi_{i-1} \\ + e^{(\phi_{i-1} - \phi_i)} \sin\phi_{i-1} - e^{(\phi_{i-1} - \phi_i)} \cos\phi_{i-1} \end{bmatrix} \end{array}\right\} \tag{7}$$

$$D_i = \frac{1}{2\psi_i}\left\{\begin{array}{l} \tilde{\delta}_i \begin{bmatrix} -2\cos\phi_i + e^{(\phi_i - \phi_{i-1})} \sin\phi_{i-1} - e^{(\phi_i - \phi_{i-1})} \cos\phi_{i-1} \\ - e^{(\phi_{i-1} - \phi_i)} \sin\phi_{i-1} - e^{(\phi_{i-1} - \phi_i)}{}_i \cos\phi_{i-1]} \end{bmatrix} \\ + \delta_{i-1} \begin{bmatrix} 2\sin\phi_{i-1} + e^{(\phi_i - \phi_{i-1})} \sin\phi_i + e^{(\phi_i - \phi_{i-1})} \cos\phi_i \\ + e^{(\phi_{i-1} - \phi_i)} \sin\phi_i - e^{(\phi_{i-1} - \phi_i)} \cos\phi_i \end{bmatrix} \\ + \Phi_{i-1} \begin{bmatrix} 2\cos\phi_{i-1} + e^{(\phi_i - \phi_{i-1})} \sin\phi_i + e^{(\phi_i - \phi_{i-1})} \cos\phi_i \\ - e^{(\phi_{i-1} - \phi_i)} \sin\phi_i + e^{(\phi_{i-1} - \phi_i)} \cos\phi_i \end{bmatrix} \\ + \Phi_i \begin{bmatrix} -2\sin\phi_i - e^{(\phi_i - \phi_{i-1})} \sin\phi_{i-1} + e^{(\phi_i - \phi_{i-1})} \cos\phi_{i-1} \\ - e^{(\phi_{i-1} - \phi_i)} \sin\phi_{i-1} - e^{(\phi_{i-1} - \phi_i)} \cos\phi_{i-1} \end{bmatrix} \end{array}\right\} \tag{8}$$

ϕ_i , ϕ_{i-1} , Ψ_i, $\tilde{\delta}_i$, Φ_i, and Φ_{i-1} are, respectively, given by the following equations:

$$\phi_i = \kappa_i\, x_i \quad , \quad \phi_{i-1} = \kappa_i\, x_{i-1} \tag{9}$$

$$\Psi_i = 2 + e^{\phi_i - \phi_{i-1}} \sin\phi_i \sin\phi_{i-1} + e^{\phi_i - \phi_{i-1}} \cos\phi_i \cos\phi_{i-1} + e^{\phi_{i-1} - \phi_i} \sin\phi_i \sin\phi_{i-1} + e^{\phi_{i-1} - \phi_i} \cos\phi_i \cos\phi_{i-1}$$

$$\tilde{\delta}_i = \frac{k_{s_i}\, \delta_i}{\kappa_i{}^3\, E\, I_{F_i}} \tag{10}$$

$$\Phi_i = \frac{k_{t_i}\, \theta_i}{\kappa_i^2\, E\, I_{F_i}} \quad , \quad \Phi_{i-1} = \frac{\theta_{i-1}}{\kappa_i} \tag{11}$$

2) Horizontal Response of Subsystem 2 (beams/floors).

Considering both damping and support motion, the normalized deflection amplitude at the interface node is given by the following equation:

$$\delta_i = \frac{r_i^2\, F_i}{k_{s_i} \sqrt{(1 - r_i^2)^2 + (2\, \xi\, r_i)^2}} \tag{12}$$

International Journal of Civil And Structural Engineering – IJCSE 2018
Copyright © Institute of Research Engineers and Doctors , SEEK Digital Library
Volume 5 : Issue 2- [ISSN : 2372-3971] - Publication Date: 28 December, 2018

where ω_i = natural frequency, Ω = forcing frequency, r_i = frequency ratio (Ω/ω_i), ξ = damping ratio, and F_i = force amplitude at the interface node i.

The net force is given by the following equation:

$$F_i = E\, I_i \left[\frac{d^3 y_i}{dx^3} - \frac{d^3 y_{i+1}}{dx^3}\right]_{x_i} \qquad (13)$$

Combining Eqs. 10, 12, and 13 yields the following equation:

$$\tilde{\delta}_i = \frac{R_i\, r_i^2}{\sqrt{(1-r_i^2)^2 + (2\,\xi\, r_i)^2}}\ \eta_i \qquad (14)$$

η_i is given by the following equation:

$$\eta_i = (A_i - A_{i+1})e^{\phi_i} - (B_i - B_{i+1})e^{-\phi_i} + (C_i - C_{i+1})\sin\phi_i - (D_i - D_{i+1})\cos\phi_i$$

where $\phi_i = \kappa_i\, x_i$

The ratio of the column stiffness to the total frame stiffness, R is given by the following equation:

$$R = \frac{I_i}{I_{Fi}} \qquad (15)$$

3) Rotational Response of Subsystem 2 (beam/floor)

Considering system damping and support motion, the rotation normalized amplitude at the interface node i is given by the following equation:

$$\theta_i = \frac{r_i^2\, M_i}{k_{t_i}\sqrt{(1-r_i^2)^2 + (2\xi\, r_i)^2}} \qquad (16)$$

The moment M_i is given by the following equation:

$$M_i = E\, I_i \left[\frac{d^2 y_i}{dx^2} - \frac{d^2 y_{i+1}}{dx^2}\right]_{x_i} \qquad (17)$$

Combining Eqs. 11, 16, and 17 yields the following equation:

$$\Phi_i = \frac{R_i\, r_i^2}{\sqrt{(1-r_i^2)^2 + (2\,\xi\, r_i)^2}}\ \hat{\eta}_i \qquad (18)$$

where $\hat{\eta}_i$ is given by the following equation:

$$\hat{\eta}_i = (A_i - A_{i+1})e^{\phi_i} + (B_i - B_{i+1})e^{-\phi_i} - (C_i - C_{i+1})\sin\phi_i - (D_i - D_{i+1})\cos\phi_i$$

4) Perturbation Procedure

The perturbation procedure [21] starts with the determination of the zero-order solution constants A_i^0, B_i^0, C_i^0, and D_i^0. The success of the perturbation procedure is highly dependent on the chosen zero-order (initial) solution. In the current work, the zero-order solution was obtained using the loading case shown in Figure 3. The selected loading case reflects an acceptable earthquake design which recommends that the beam-column connections be rigid and that flexural hinges form in beams rather than in columns.

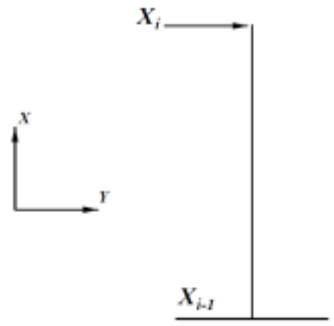

Figure 3: Free End Loading Model

This loading case leads to the following boundary conditions at the interface nodes:

At point x_{i-1}: $y_i = \delta_{i-1} = 1$ $\qquad \frac{1}{\kappa_i}\frac{dy_i}{dx} = 0$

At point x_i: $E\, I_{F_i}\frac{d^3 y_i}{dx^3} = 0$ $\qquad E\, I_{F_i}\frac{d^2 y_i}{dx^2} = 0$

Applying these boundary conditions to Eq. 3 yields the following zero-order constants A_i^0, B_i^0, C_i^0, and D_i^0:

$$A_i^0 = \frac{1}{2\psi_i}\{e^{-\phi_{i-1}} + e^{-\phi_i}\sin\phi_i\sin\phi_{i-1} + e^{-\phi_i}\cos\phi_i\sin\phi_{i-1} + e^{-\phi_i}\sin\phi_i\cos\phi_{i-1} + e^{-\phi_i}\cos\phi_i\cos\phi_{i-1}\}$$

$$B_i^0 = \frac{1}{2\psi_i}\{e^{-\phi_{i-1}} + e^{-\phi_i}\sin\phi_i\sin\phi_{i-1} - e^{-\phi_i}\cos\phi_i\sin\phi_{i-1} + e^{-\phi_i}\sin\phi_i\cos\phi_{i-1} + e^{-\phi_i}\cos\phi_i\cos\phi_{i-1}\}$$

$$C_i^0 = \frac{1}{2\psi_i}\{-2\cos\phi_{i-1} - e^{(\phi_i-\phi_{i-1})}\sin\phi_i + e^{(\phi_i-\phi_{i-1})}\cos\phi_i + e^{(\phi_{i-1}-\phi_i)}\sin\phi_i + e^{(\phi_{i-1}-\phi_i)}\cos\phi_i\}$$

$$D_i^0 = \frac{1}{2\psi_i}\{2\sin\phi_{i-1} + e^{(\phi_i-\phi_{i-1})}\sin\phi_i + e^{(\phi_i-\phi_{i-1})}\cos\phi_i + e^{(\phi_{i-1}-\phi_i)}\sin\phi_i - e^{(\phi_{i-1}-\phi_i)}\cos\phi_i\}$$

The computed zero-order constants A_i^0, B_i^0, C_i^0, and D_i^0 are then used to determine the first-order responses of both subsystems (i.e., columns and beams). The first-order response $y_i^{(1)}$ of all columns are computed using Eq. 3. After that, the horizontal responses of the beam are determined using Eq. 14 while the rotational responses are determined using Eq. 18.

In the next step, the first-order constants A_i^1, B_i^1, C_i^1, and D_i^1 are computed using Equations; 5, 6, 7, and 8. These constants

International Journal of Civil And Structural Engineering – IJCSE 2018
Copyright © Institute of Research Engineers and Doctors , SEEK Digital Library
Volume 5 : Issue 2- [ISSN : 2372-3971] - Publication Date: 28 December, 2018

are then used to compute the second-order responses $y_i^{(2)}$ of all columns.
The same computational procedure is repeated until the convergence of the perturbation series is reached.

2. Program Flowchart

A computer program has been written in Quick Basic to implement the structure mixture theory procedure. The program computational algorithm is shown in Figure 4.
The first step of the program consists of reading the input data. The second step of the program involves the computation of the structure natural frequencies and corresponding mode shapes. The computation is performed as follows.

1) Assemble the structure mass and stiffness matrices.
2) Calculate the natural frequencies and corresponding mode shapes using Jacobi's method.

The third step of the program includes the following computation tasks for each forcing frequency:

1. The wave numbers, κ_i, is computed using Eq. 2.
2. The zero-order solution constants A_i^0, B_i^0, C_i^0, and D_i^0 are computed.
3. The first-order responses $y_i^{(1)}$ of the column sections are computed using Eq. 3. The horizontal and rotational responses of the beams are then computed using Equations; 5 and 7, respectively.
4. The first-order solution constants A_i^1, B_i^1, C_i^1, and D_i^1 are computed.
5. Steps 3 and 4 are repeated until the perturbation series converges.
6. The final nodal displacements δ_i and slopes θ_i are determined at the beam/column interfaces.
7. The maximum amplitudes y_{0i} are computed using the following equation:

$$y_{o_i} = \frac{Fo_i}{K_i\sqrt{1+(2*r_i*\xi)^2}} \qquad (19)$$

where Fo_i = nodal static load, K_i = frame shear stiffness, r_i = frequency ratio, and ξ = damping ratio of the frame.

8. The modal participation factors Γ_i are computed using the following equation:

$$\Gamma_i = \sum_{j=1}^{n} M_j a_{ij} \qquad (i = 1,2,.....n) \qquad (20)$$

where n = number of nodes (floors), [M] = structural mass matrix, and [a] = mode shape matrix.

9. The expected nodal deflections are computed using a modified SRSS method (Paz 1991) as follows.

$$u_i = \sqrt{\sum_{j=1}^{n} (\Gamma_i a_{ij} \delta_j)^2} * y_{o_i} * \frac{1}{R_i} \qquad (21)$$

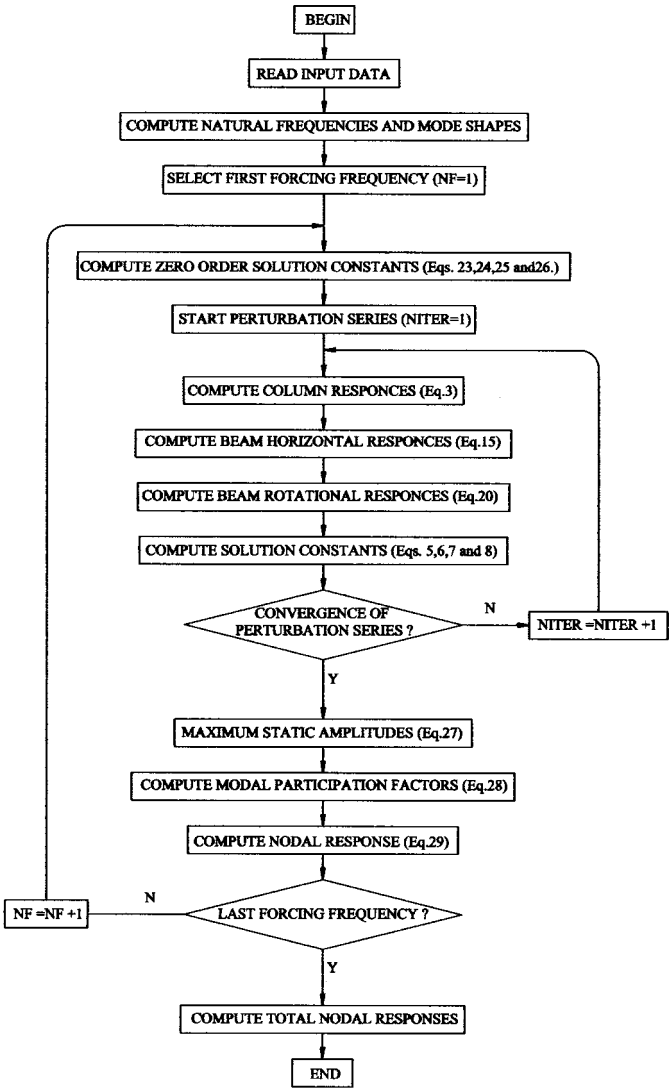

Figure 4: Structure Mixture theory Computational Flowchart

10. Finally, the total nodal responses are found by adding the results obtained in Step 9 for all forcing frequencies using the following equation:

$$u_{T_i} = \sum_{j=1}^{NF} u_j \qquad (22)$$

where NF = number of forcing frequencies.

3. Program Input Data

The program input data consists of three parts. The first part contains the following general input information: number of nodes (floors), number of forcing frequencies, maximum number of iterations, and convergence tolerance. The second part of the input data includes the following structural model information: Total building height, story heights, story beam-column stiffness ratios (I_i/I_{Fi}), wave propagation factors ($c\, r_{gi}$), story total stiffness ($E\, I_i$), and floor masses. The third part of

International Journal of Civil And Structural Engineering – IJCSE 2018
Copyright © Institute of Research Engineers and Doctors , SEEK Digital Library
Volume 5 : Issue 2- [ISSN : 2372-3971] - Publication Date: 28 December, 2018

the input data includes the forcing frequencies, th corresponding nodal damping ratio (ξ), and the maximur nodal static loads (Fo).

4. Program Output Data

The program output data consists of four parts. Th first part contains the vertical and torsional expansio parameters. The second part includes the following noda amplitude information: forcing frequency, number c iterations, node numbers, and nodal amplitudes. The thir part includes the static displacement information consisting c forcing frequencies, floor numbers, and static noda displacements. The fourth part includes the floc displacements for each forcing frequency and the total floc displacements.

5. Case Study #1

In the first case study, the experimental earthquak responses of a full-size two-story reinforced concrete buildin were compared to those obtained using the structure mixtur theory. The building was tested at the University of Californi at Berkeley under a National Science Foundation researc project grant. Figures 5 and 6 shows the front and sid elevation of the test structure, respectively. Table summarizes the structural model input data. Three simulate earthquakes, labeled W1, W2, and W3 were applied to the tes structure. Table 2 summarizes the peak input ground acceleration, damping, and dominant forcing frequencies for the tests W1, W2, and W3.

Table 1: Structural model input data for two story building

Building	*Floor Number*	*Floor Height (m)*	*Floor Mass (kg)*	*Floor Shear Stiffness (kN/m)*	*Floor Stiffness Ratio (I/I_F)*	*Wave Propagation Factor (C rg) (m^2/s)*
Two-Story	1	5.7	10010	5347	0.5	173
	2	6.2	6160	4213	0.5	173

Table 3 summarizes the maximum roof displacements obtained using the structure mixture theory as well as those obtained experimentally. The roof displacements obtained using the structure mixture theory were compared to those obtained experimentally. The average absolute percent difference and the maximum absolute percent difference between the roof displacements obtained using the structure mixture theory and those obtained experimentally are equal to 3.5% and 7.2% (test W2), respectively. This shows that the structure mixture theory results are close to those obtained experimentally.

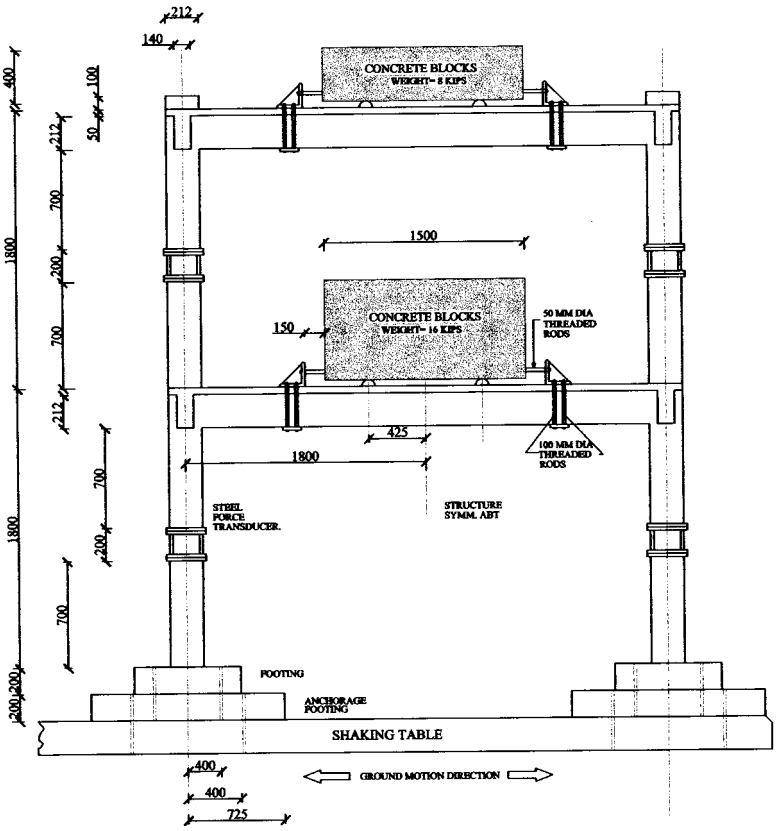

FRONT ELEVATION

Figure 5: Test Structure and Test Arrangement
All dimensions are in (mm)

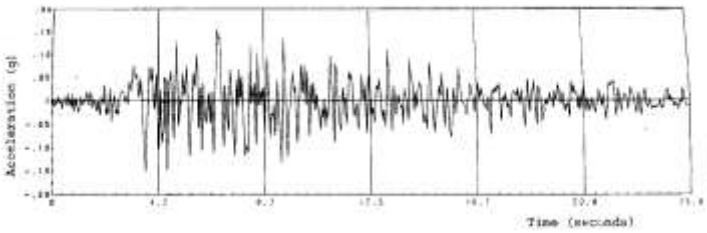

Figure 6: Input ground motion for tests W1, W2 and W3

Table 2: Peak ground acceleration, damping and forcing frequency for W1, W2 and W3

Test	*Input Signal*	*Ground Acceleration (% g)*	*Percent Damping (%)*	*Dominant Forcing Frequency (Hz)*
W1	TAFT N69W	9.7	2	2.53
W2	TAFT N69W	57.0	2	2.53
W3	TAFT N69W	65.0	2	2.53

International Journal of Civil And Structural Engineering – IJCSE 2018
Copyright © Institute of Research Engineers and Doctors , SEEK Digital Library
Volume 5 : Issue 2- [ISSN : 2372-3971] - Publication Date: 28 December, 2018

Table 3: Maximum experimental and computed lateral displacements for Case Study-1

Test Number	*Experimental Maximum Displacements (mm)*	*Computed Maximum Displacements (mm)*
W1	11.0	11.1
W2	69.2	64.2
W3	70.4	72.1

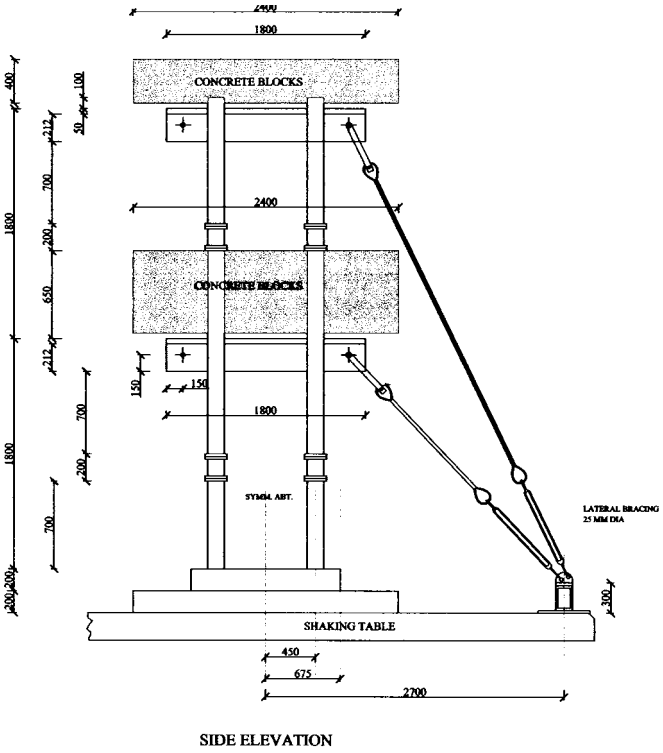

Figure 7: Test Structure and Test Arrangement
(All dimensions are in (mm)

6. CASE STUDY #2

In the second case study, the experimental earthquake responses of a full-size seven story reinforced concrete building were compared to those obtained using the structure mixture theory. The building was tested as part of the US-Japan Cooperative Earthquake Program (ACI, 1985). Figure 8 shows a general plan view of the building while Figure 9 shows a general elevation of the building (frame B). The central frame has a shear wall in the central bay which is continuous from the first through the seventh story.

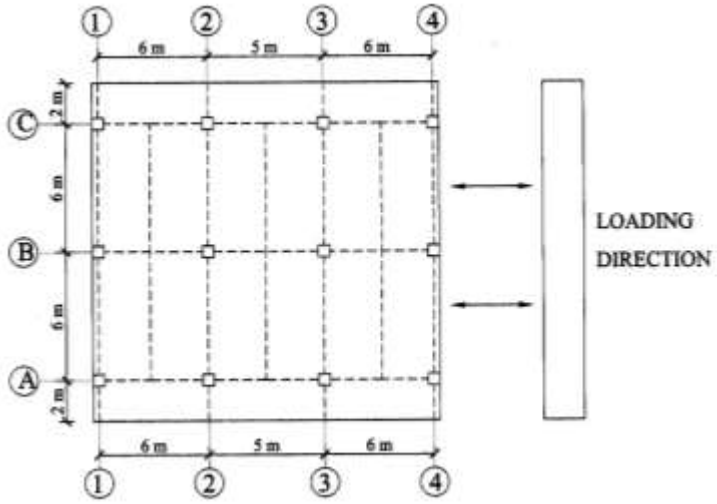

Figure 8: General Plan View of Seven Story Building

The column dimensions are 500 mm x 500 mm throughout the structure. The dimensions of the girders parallel to the loading direction are 300 mm x 500 mm from the second to the roof level. The shear wall parallel to the loading direction has a thickness of 200 mm. The floor slabs have a thickness of 120 mm throughout the structure. Table 4 summarizes the structural model input data.

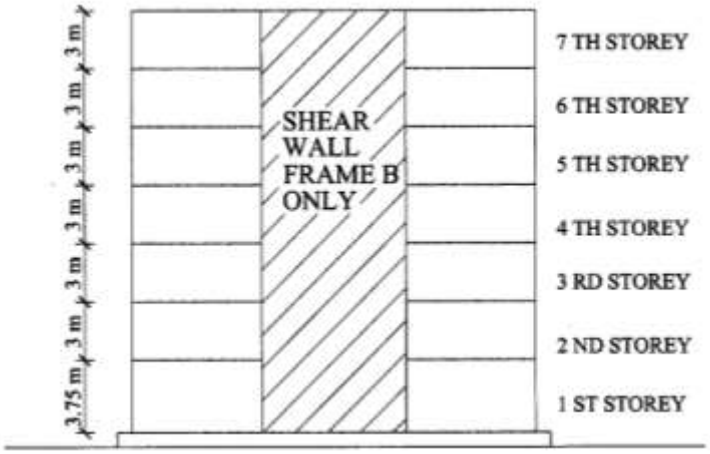

Figure 9: General Elevation of Seven Story Building (SP-84, 1985)

Table 4: Structural model input data for seven-story building

Floor Number	*Floor Height* (m)	*Floor Mass* (kg)	*Floor Shear Stiffness* (kN/m)	*Floor Stiffness Ratio* (I/I_F)	*Wave Propagation Factor* (C_{rg}) (m^2/s)
1	3.75	182700	222400	0.08	447
2-6	3.00	177300	439700	0.08	447
7	3.00	136000	439700	0.08	447

A simulated ground motion test, labeled SPD-1 was applied to the test structure. Figure 10 shows the test input ground motion while Figure 11 shows the fast Fourier transform of the test input ground motion acceleration. Table 5 summarizes the peak input ground acceleration, damping, and forcing frequencies for the test.

Table 6 summarizes the maximum roof displacement for the building obtained using the structure mixture theory as well as that obtained experimentally. The roof displacement obtained using the structure mixture theory was compared to the one obtained experimentally. The absolute percent difference between the roof displacement obtained using the structure mixture theory and that obtained experimentally is equal to 3.2%. This shows that the structure mixture theory result is close to the experimental result.

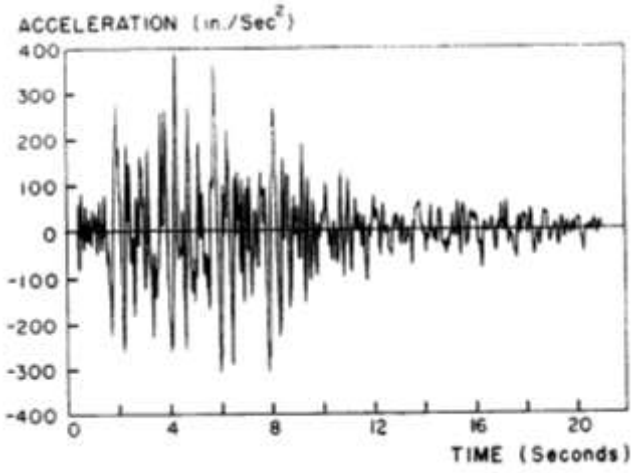

Figure 10: Input ground motion for SPD-1

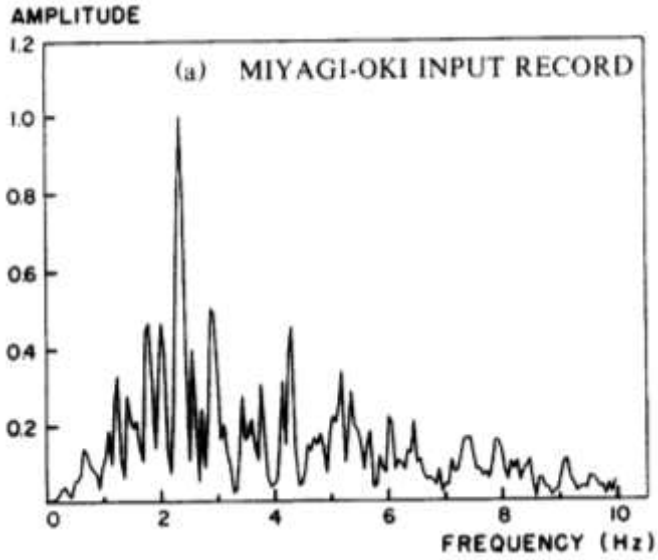

Figure 11: Fast Fourier transform of input ground acceleration for the SPD-1 test

Table 5: Peak ground acceleration, damping, and forcing frequency for SPD-1.

Test	*Input Signal*	*Ground Acceleration* (% g)	*Percent Damping* (%)	*Dominant Forcing Frequency* (Hz)
SPD-1	Miyagi-Oki	2.40	2.1	1.82

Table 6: Maximum Experimental and computed lateral displacements for Case Study -2

Test Number	*Experimental Maximum Displacements* (mm)	*Computed Maximum Displacements* (mm)
SPD-1	2.5	2.56

7. CASE STUDY #3

The steel frame shown in Figure 12a is subjected to a ground motion depicted in Figure 12b, and the maximum response of the frame at the girder level is determined. The solution steps for this example are as follows;

International Journal of Civil And Structural Engineering – IJCSE 2018
Copyright © Institute of Research Engineers and Doctors , SEEK Digital Library
Volume 5 : Issue 2- [ISSN : 2372-3971] - Publication Date: 28 December, 2018

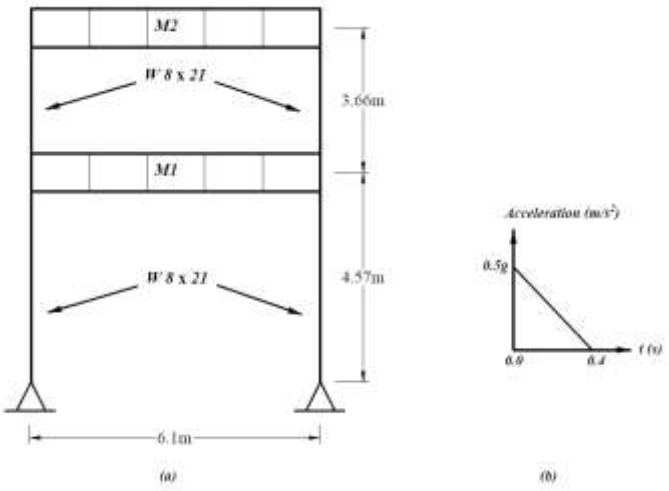

Figure 12: Idealized Structure and Loading

1- Model the structure as two degrees of freedom, determine the natural frequencies and corresponding normal frequencies and corresponding normalized modes, as shown in Table -7.

2- Use a computer program to calculate the acceleration and displacement at each $\Delta t = 0.005;$ here, the program will utilize the $Wilson - \theta$ method with $\theta = 1.4$ (Figure-13 is a plot showing the changes of acceleration with respect to the time).

3- Apply fast Fourier transform to the acceleration data obtained from step-2, and use the parameters in Table 8 to determine the forcing frequency as shown in Figure 14.

$$\Omega_1 = 1.532\ hz; \qquad \Omega_2 = 1.900\ hz$$

4- Maximum amplitude

$$y_o = \frac{F_o}{K\sqrt{1+(2\ x\ r\ x\ \xi)^2}} \qquad (23)$$

Table 9 will show the changes in $y_o$corresponding to the ratios of forcing frequencies to the natural frequencies.

5- Use the participating factor to calculate the effects of each node with respect to the other nodes of the model in the process of calculating the total deflection of each node.

$$\Gamma_i = \sum_{j=1}^{n} M_j a_{ji}\ (i = 1,2,\ldots.n) \qquad (24)$$

$$\Gamma_1 = M_1 a_{11} + M_2 a_{21} = 4.9605$$

6- The nodal deflection amplitudes have been calculated using the structural mixture theory program. The nodal deflection amplitudes and the relating frequencies are shown in Table 10.

7- Once the modal deflection amplitudes of each node are obtained, calculate the expected response of each node, based on the structural mixture theory approach, by modifying the SRSS method [9].

$$U_{imax|\Omega} = \sqrt{\sum_{j=1}^{n}(\Gamma_i a_{ij} v_j)^2} \times y_o \times \frac{1}{R} \qquad (25)$$

$$U_{1max|\Omega=1.532} = \sqrt{\left(\begin{matrix}4.9605\\ \times 0.17794\\ \times 0.139\end{matrix}\right)^2 + \left(\begin{matrix}0.62695\\ \times 0.18709\\ \times 0.004\end{matrix}\right)^2}$$

$$\times 31.59\ \times 2 = 7.77\ mm$$

$$U_{2max|\Omega=1.532} = \sqrt{\left(\begin{matrix}4.9605\\ \times 0.22914\\ \times 0.139\end{matrix}\right)^2 + \left(\begin{matrix}0.62695\\ \times -0.21794\\ \times 0.004\end{matrix}\right)^2}$$

$$\times 31.63\ \times 2 = 10.02\ mm$$

$$U_{1max|\Omega=1.900} = \sqrt{\left(\begin{matrix}4.9605\\ \times 0.17794\\ \times 0.544\end{matrix}\right)^2 + \left(\begin{matrix}0.62695\\ \times 0.18709\\ \times 0.014\end{matrix}\right)^2}$$

$$\times 13.11\ \times 2 = 12.66\ mm$$

$$U_{2max|\Omega=1.900} = \sqrt{\left(\begin{matrix}4.9605\\ \times 0.2914\\ \times 0.544\end{matrix}\right)^2 + \left(\begin{matrix}0.62695\\ \times -0.21794\\ \times 0.0142\end{matrix}\right)^2}$$

$$\times 13.13\ \times 2 = 16.24\ mm$$

8- The total displacement of each node is;

$$u_{1\,total} = 7.77 + 12.6 = 20.37\ mm$$

$$u_{2\,total} = 10.02 + 16.24 = 26.26\ mm$$

9- Compare the maximum displacement from step 2 with the displacement calculated in step 7. Table 11 will show the comparison.

Table 7: Parameters and Vibration properties of Structure

Parameters	*First Story*	*Second Story*	*Remarks*
Mn	2,627 $N.s^2/m$	1,751 $N.s^2/m$	Mass
Kn	406,974 *N/m*	653,366 *N/m*	Stiffness Coefficient
ξ	0.05	0.05	Damping Ratio
Cn	3,269 $N.s^2/m$	3,383 $N.s^2/m$	Damping Coefficient
ω_m	2.91 hz *(1st mode)*	8.4 hz *(2nd mode)*	Natural frequency
a_{mn}	a_{11}=0.178 a_{12}=0.229	a_{11}=0.187 a_{12}=0.217	Normalized mode shapes *m* => mode number *n* => node number

Table 8: Parameters of FFT

N=data number	*M=0,1,… N/2*	$\Delta f=(1)/(N\Delta T)$	$f_{max}=(1)/(N\Delta T)$	**Remarks**
80	0,1,….40	2.5	100	$f_{max}=(m)/(N\Delta T)$ *hz*

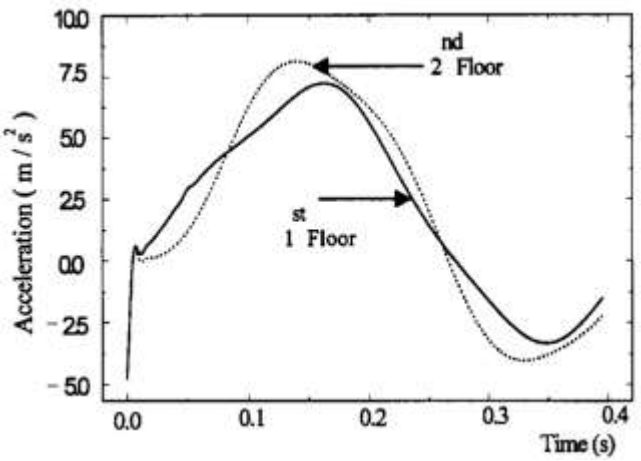

Figure 13: Time vs Acceleration at Node from Wilson -θ Method

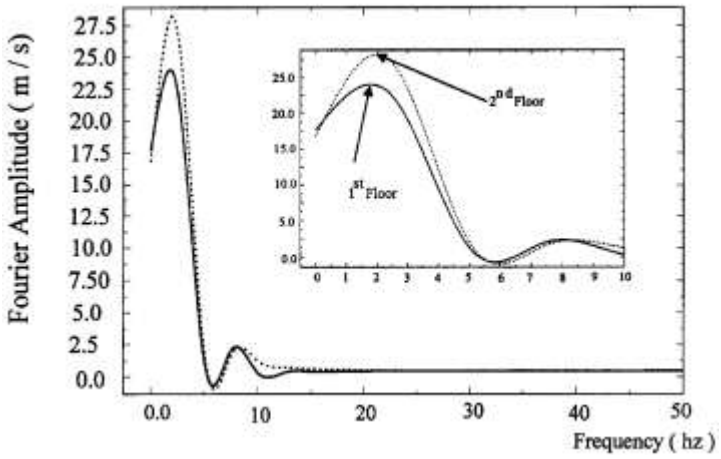

Figure 14: Fourier Amplitude Spectrum of Ground Acceleration

Table 9: Maximum Amplitude

ω *(cps)*	Ω *(cps)*	$r=\Omega/\omega$	y_o *(mm)*
2.91	1.532	0.52646	31.59
8.4	1.532	0.18238	31.631
2.91	1.9	0.652921	13.11
8.4	1.9	0.226190	13.13

Table 10: Structural Mixture Theory Nodal Deflection Amplitude

ω *(cps)*	Ω *(cps)*	*v (m/s)*
2.91	1.532	0.139
8.4	1.532	0.004
2.91	1.9	0.544
8.4	1.9	0.014

Table 11: Comparison Table

Response (mm)	*Wilson –θ*	*Mixture theory*
U_1	20.25	20.36
U_2	25.63	26.26

8. CASE STUDY #4

This example the observed earthquake response of a nine story steel frame building during the San Fernando earthquake and compared with the structural mixture theory (SMT) numerical results of the structure. The forcing frequencies of the real earthquake will be used in the SMT calculation.

The Jet Propulsion Laboratory (JPL) building is a nine story building modeled as an eight story building (Figure 15). For more details of the building refer to [20]. To determine the total maximum roof displacement of the building in the east-west direction, the solution steps for this example are as follows:

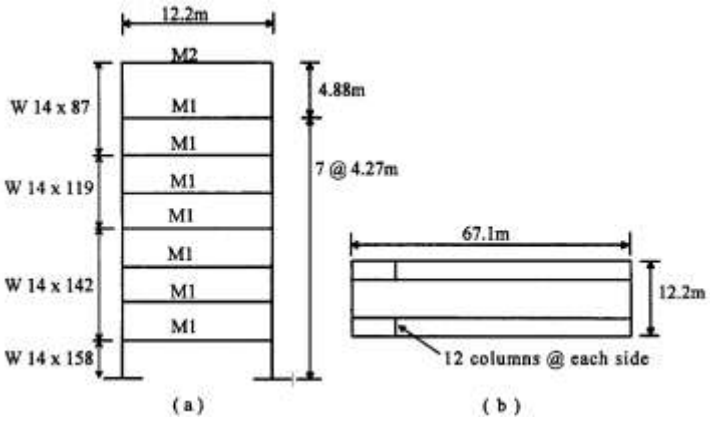

Figure 15: Idealized Structure and Loading of JPL Building

1- Model the structure with eight degrees of freedom; determine the natural frequencies and corresponding normalized modes as mentioned in Table 12.

2- The nodal deflection amplitudes have been calculated using the structural mixture theory program, See the nodal deflection amplitudes and relating frequencies in Table -13.

3- Refer to the roof maximum amplitude shown in Table-14.

4- Once the modal deflection amplitudes of each node are obtained, the expected response of each node based on the structural theory approach is calculated by modifying the SRSS method, and calculated response is shown in Table -15.

Table 12: Structural Mixture Theory Nodal Deflection Amplitude of Roof

ω (cps)	Ω (cps)	v (m/s)
0.856402	0.78	7.95 E-03
2.25427	0.78	4.91 E-03
3.61813	0.78	2.29 E-03
4.99634	0.78	1.46 E-04
6.10531	0.78	5.48 E-04
7.40036	0.78	5.22 E-04
8.34175	0.78	4.16 E-04
9.37115	0.78	-7.81 E-08
0.856402	2.4	-6.94 E-03
2.25427	2.4	1.6
3.61813	2.4	-0.082
4.99634	2.4	1.05 E-03
6.10531	2.4	8.19 E-03
7.40036	2.4	6.84 E-03
8.34175	2.4	-2.01 E-02
9.37115	2.4	1.57 E-03
0.856402	3.85	1.14 E-03
2.25427	3.85	4.28 E-02
3.61813	3.85	0.135
4.99634	3.85	5.72 E-02
6.10531	3.85	7.44 E-02
7.40036	3.85	-1.26 E-02
8.34175	3.85	8.20 E-03
9.37115	3.85	-5.85 E-05

Table 13: Parameters and Vibration Properties of Structure

Node	***1***	***2***	***3***	***4***	***5***	***6***	***7***	***8***	***Remarks***
ω_m	0.8564	2.254	3.618	4.996	6.105	7.4	8.341	9.37	Natural frequencies (hz)
a_{8n}	0.00905	0.00956	-0.00730	-0.00466	0.00232	-0.00076	-0.00021	-0.00003	Roof normalized mode shapes
Γ_n	148.41	-52.87	-31.814	22.15	17.573	12.838	-8.814	6.3963	Participation Factors
Ω_n	0.78	2.40	3.85	---	---	---	---	---	Forcing Frequencies (hz)
ξ_n	0.04	0.06	0.06	---	---	---	---	---	Damping Ratio
Acceleration	13	21	9	---	---	---	---	---	Maximum roof acceleration (%g)
u_8	---	---	---	---	---	---	---	63.5	Maximum total roof displacement (mm)

Table 14: Roof Maximum Amplitude

ω ***(cps)***	**Ω** ***(cps)***	$r = \Omega/\omega$	y_o ***(mm)***
9.37115	0.78	0.083234	23.39
9.37115	2.4	0.256105	37.77
9.37115	3.85	0.410835	16.18

Table 15: Maximum Displacement of Roof

Ω ***(cps)***	u_8 ***(mm)***
0.78	5.00
2.4	61.02
3.85	1.23

5- The maximum total displacement is

$$u_{8\,total} = 5 + 61.02 + 1.23 = 67.27\ mm$$

6- Comparison of the maximum total roof displacement (63.5mm) from earthquake records with the calculated roof displacement (67.27mm) by the structural mixture theory showed that the result is relatively very good.

9. CONCLUSION

Four case studies were conducted to evaluate the performance of the structure mixture theory in the earthquake response analysis of buildings. In the first case study, the actual earthquake responses of a two-story reinforced concrete building, which was tested at the University of California at Berkeley, were compared to those obtained using the structure mixture theory. In the second case study, the actual earthquake responses of a seven-story reinforced concrete building, which was tested as a part of the US-Japan Cooperative Earthquake Program, was considered. The third case study is about the calculation of nodal deflection amplitude with SMT and comparison of the results obtained from Wilson-θ method. In the fourth case study, the observed earthquake response of a nine-story steel frame building during San Fernando earthquake is compared with the SMT numerical results of the structure. The experimental and numerical results were found to be close to those obtained using the structure mixture theory in all of the four case studies. The mean differences between the maximum roof displacements obtained experimentally for the three case studies (Case-I, II and IV) and those obtained using the structure mixture theory were found to be equal to 3.5%, 3.2%, 2.4% and 5.6% respectively. These results indicate that the performance of the structure mixture theory is adequate in the earthquake analysis of multi-story buildings. These results indicate that the performance of the structure mixture theory is adequate in the earthquake analysis of multi-story buildings.

This research has also led to the verification of a structural mixture theory that can be used to predict the response of a structural frame to earthquake ground motion. In the section

on the theoretical development, the analysis of the response proceeded by formulating and solving a set of governing equations subjected to boundary conditions at the interface points joining two subsystems; the supporting columns and the cross beams/flooring of the structure. The boundary conditions include damping ratios, moment of inertia ratios, frequency ratios, and support motion effects. The analysis uses the structural mixture theory model of the total structure as being composed of the two interacting subsystems

In Case -III, an example of the numerical results of the structural mixture theory is given, showing a good agreement with the result of the more standard Wilson – θ method.

Several conclusions about the structural mixture theory may be drawn from this research.

1- The choice of the flexural wave beam equation to govern the response of the columns (subsystem 1) yields good results.

2- The theory yields good estimates of the nodal deflection amplitudes.

3- The matching boundary conditions at the subsystem interface, and the conditions leading to zero-order solution must be chosen carefully.

4- The theory can be used to determine the response of either SDOF or MDOF structures to earthquake ground motion, given that they confirm to the model of two interacting subsystems.

5- The theory is sensitive to the value of the forcing frequency. The calculation yields better results when the determined forcing frequency is close to the actual forcing frequency.

6- The moment-of-Inertia ratio, R, Plays an important role in the convergence of the perturbation calculations.

7- At each step of the perturbation procedure of the structural mixture theory, the nodal forces F_i, and the nodal moments M_i are computed using the nodal displacement δ_i and the nodal rotations θ_i using Eqn. (13) and (18), respectively. This computational procedure allows for the consideration of the additional nodal forces and moments due to $P-\Delta$ effects.

Some advantages of the structural mixture theory over other methods in calculating the response of MDOF structures are that initial conditions, time integration, and spectral charts are not needed. Also the computer damping matrix for the structure is not needed, given that the modal damping ration is known.

Further research is necessary to investigate the use of other equations of motions in conjunction with the structural mixture theory, including equations governing the response of plates and shells. The effects of foundations and soil conditions should be studied and included in the model if possible. The model should be generalized for application to space frames and other three- dimensional structures. And finally, the application of the structural mixture theory to the nonlinear behavior of structures should be explored.

10. REFERENCES

[1] Al-Ansari, M. S., Kirkely O. M., and Gillette, G. (1996). "Earthquake response of structures by structural mixture theory" *J. Struct. Engrg., American Society of Civil Engineers*, Vol. 122 (10), 1198-1207.

[2] Filiatrault A., Lachapelle E., and Lamontagne P. (1998). "Seismic performance of ductile and nominally ductile reinforced concrete moment resisting frames. II. Analytical study", *Canadian Journal of Civil Engineers*, Vol. 25(2).

[3] ACI (1995). *Building code requirements for structural concrete*, ACI 318-89, American Concrete Institute, Detroit, MI.

[4] Clough, R.W. and Jawahar Gidwani (1976). "Reinforced concrete frame 2: seismic testing and analytical correlation." Report No. EERC 76-15, Earthquake Research Center, College of Engineering, University of California, Berkeley, CA.

[5] M. S. Al-Ansari (2009), "Tall building configuration effects on their response to earthquake loading, Journal of Civil Engineering and Architecture, May 2009, Volume 3, No.5, ISSN 1934-7359, USA.

[6] Sazzad, Md. Mahmud & Azad, Md. Samdani. (2015), "Effect of building shape on the response to wind and earthquake" International journal of advanced structures & geotechnical engineering, ISSN 2319-5347, Vol. 04, No. 04, 2015.

[7] Bergman, L. A., and Nicholson, J. W. (1985). "Forced vibration of a damped combined linear system." J. Vibration Acoustics, Stress, and Reliability in Des, 107, 275-281.

[8] Hao Chen, Quancai Xie, Biao Feng, Jinlong Liu, Yong Huang & Hongfu Chen (2018), "Seismic Performance to Emergency Centers, Communication and Hospital Facilities Subjected to Nepal Earthquakes, 2015", Journal of Earthquake Engineering, Vol. 22, Issue 9, ISSN 1537-1568.

[9] Baiping Dong, Richard Sause and James M. Ricles (2018), "Seismic Response and Damage of Reduced-Strength Steel MRF Structures with Nonlinear Viscous Dampers", Journal of Structural Engineering (ASCE) Vol. 144, Issue 12 2018.

[10] Memari, A., Motlagh Y. A. R., Akhtari M., Scalon A., Ashtiany G. M. (1999). "Seismic vulnerability evaluation of a 32-story reinforced concrete building," *Structural Engineering and Mechanics*, Vol. 7(1).

[11] Stephen, R. M., Wilson, E. L., and Stander, N. (1985). "Dynamic properties of a thirty-story condominium tower building," *Earthquake Engineering Research Center*. Report No. EERC-85/03, Berkeley, CA.
[12] NBCC (1995). National Building Code of Canada, Associate Committee on the National Building Code, National Research Council of Canada, Ottawa, Ontario.
[13] UBC (1994). *International Conference of Building Officials, Uniform Building Code*, Vol. 2, ICBO, Whittier, California, 1994.
[14] Paz, M. B. (1991). *Structural dynamics theory and computation*. Van Nostrand Reinhold, New York, N.Y.
[15] Craig, R. R. (1981). Structural dynamics. John Wiley & Sons, Inc., New York, N.Y.
[16] M. S. Al-Ansari (2011), "Formulating building response to Earthquake loading", International Journal of Civil and Structural Engineering ,Volume 2, No 1, 2011, ISSN 0976 – 4399
[17] M. S. Al-Ansari (2009), "Tall building configuration effects on their response to earthquake loading, Journal of Civil Engineering and Architecture, May 2009, Volume 3, No.5, ISSN 1934-7359, USA.
[18] Wilson, E. L., Farhoomand, I., and Bathe, K. J. (1973). "Nonlinear dynamic analysis of complex structures." Int. J. Earthquake Engr and Struct. Dynamics, Vol. I, 241-252.
[19] K. Ghaedi, Z. Ibrahim, M. Jameel, A. Javanmardi, and H. Khatibi (2018) "Seismic Response Analysis of Fully Base-Isolated Adjacent Buildings with Segregated Foundations". Advances in Civil Engineering, Vol. 2018, ID, 4517940.
[20] Wood, J. H. (1973). "Analysis of the earthquake response of a nine story steel frame building during the San Fernando Earthquake." Rep. No. EERL 72-04, California Inst of Technol., Pasadena, Calif.
[21] Gillette, G. (1991). "Coupled perturbation series for disparate mixtures." *J. Acoustical Soc. Am*., 89, 2084-2092

About Author (s):

Dr. Mohammed Salam Al-Ansari
Associate Professor,
Department of Civil and Architectural Engineering.
Qatar University

Muhammad Shekaib Afzal
Teaching Assistant,
Department of Civil and Architectural Engineering.
Qatar University